Delayed Excitations Induce Polymer Looping and Coherent Motion

Andriy Goychuk,[1,*] Deepti Kannan,[2] and Mehran Kardar[2,†]
[1]Institute for Medical Engineering and Science, Massachusetts Institute of Technology, Cambridge, Massachusetts 02139, USA
[2]Department of Physics, Massachusetts Institute of Technology, Cambridge, Massachusetts 02139, USA

(Received 29 January 2024; revised 25 June 2024; accepted 12 July 2024; published 15 August 2024)

We consider inhomogeneous polymers driven by energy-consuming active processes which encode temporal patterns of athermal kicks. We find that such temporal excitation programs, propagated by tension along the polymer, can effectively couple distinct polymer loci. Consequently, distant loci exhibit correlated motions that fold the polymer into specific conformations, as set by the local actions of the active processes and their distribution along the polymer. Interestingly, active kicks that are canceled out by a time-delayed echo can induce strong compaction of the active polymer.

DOI: 10.1103/PhysRevLett.133.078101

The conformational statistics of a biopolymer determine its function. In thermal equilibrium, sequence-specific heteropolymers explore a potential landscape [1–6] where the entropic cost of folding is compensated for by monomer-monomer and monomer-solvent interactions [7–9]. Similar ideas were used in studies of chromatin, a large heteropolymer consisting of genomic DNA and associated proteins [10]. However, chromatin also undergoes adenosine triphosphate (ATP) dependent nonequilibrium fluctuations [11] and coherent motion [12–14]. Similar to other chemically active systems [15], metabolites such as ATP fuel the cycling of chromatin-associated proteins [16–18], such as SMC complexes and remodelers, between distinct (e.g., ATP- versus ADP-bound) states with different chromatin interactions. The resulting molecular motor and biochemical activity of chromatin-associated proteins, and active fluctuations in the chromatin potential landscape, act as local excitations (kicks) out of thermal equilibrium.

The magnitude of the active kicks at each locus is set by the local energy consumption rate, implying a nonuniform activity profile which can lead to polymer folding [19]. From contact frequency data alone, polymers folded by active kicks cannot be discerned from polymers folded by additional Hookean springs [19–21], suggesting that energy-consuming processes could be absorbed into effective interaction parameters [22,23]. However, as observed for chromatin [11–14], ATP consumption substantially enhances dynamic fluctuations [24,25]. The corresponding mechanical stresses propagate via the backbone [26,27], through chemical interactions among non-neighboring monomers [23,28–30], or via the surrounding fluid [31,32], and thereby coordinate the motion of different chromosomal loci. Here, we study how the interplay between sequence-specific active kicks and stress propagation can induce correlated motions and folding.

Active kicks can originate, for example, from chemical reaction cycles, binding and unbinding of molecular motors [33], motor activity [27,31,34–36], or persistent active motion of specific loci [29,30,37–51] featuring biomolecular condensates [52–57]. To account for the unique temporal signatures of different active processes, we develop a framework where each (coarse-grained) monomer of the chain could experience kicks with different temporal correlations. Hence, unlike the well-known case where the polymer consists of identical active Brownian particles, each monomer could have a distinct velocity, persistence time, or show even more intricate memory including antipersistent motion. We show that temporal sequences of active kicks lead to sequence-specific correlated motions without relying on long-ranged couplings via bulk concentration or electrostatic potential gradients [19]. For persistent kicks with exponential memory, in addition to activity-induced bending, the polymer expands (contracts) if the excitations propagate farther (less) than the polymer's persistence length within the duration set by the memory. For antipersistent excitations where each kick is canceled out by a negative echo (that is, an active elastic recoil) we find that the active polymer is compacted much more strongly than by persistent kicks. Our analysis provides novel perspectives toward the understanding of active polymers such as chromatin.

Toward a theoretical framework for such inquiry, we idealize the polymer as a space curve $\boldsymbol{r}(s,t)$ parametrized by dimensionless material coordinates $s \in [-L/2, L/2]$. Tension propagates along the polymer via lateral stretching modes or via transversal bending modes, as captured by the energetics of an inhomogeneous wormlike chain with Kuhn length b. Assuming dissipative relaxation over a microscopic monomer diffusion time τ_b, and excitations captured

*Contact author: andriy@goychuk.me
†Contact author: kardar@mit.edu

through a random velocity field $\boldsymbol{\eta}(s,t)$, the polymer dynamics are described by

$$\tau_b[\partial_t \boldsymbol{r}(s,t) - \boldsymbol{\eta}(s,t)] = \partial_s[\kappa(s)\partial_s \boldsymbol{r}(s,t)] - \frac{1}{4}\partial_s^4 \boldsymbol{r}(s,t). \quad (1)$$

The excitations, $\boldsymbol{\eta}(s,t) \coloneqq \boldsymbol{\eta}_p(s,t) + \boldsymbol{\eta}_a(s,t)$, feature independent and identically distributed (i.i.d.) thermal kicks $\boldsymbol{\eta}_p(s,t)$ with covariance $\langle \boldsymbol{\eta}_p(s,t)\cdot\boldsymbol{\eta}_p(s',t')\rangle = 2b^2/\tau_b\delta(s-s')\delta(t-t')$, as well as active kicks $\boldsymbol{\eta}_a(s,t)$. In the thermal equilibrium limit, the above wormlike chain has steady-state tangent-tangent correlations decaying as $\langle \boldsymbol{\tau}(s,t)\cdot\boldsymbol{\tau}(s',t)\rangle = e^{-|s-s'|/l_p}$, with $\boldsymbol{\tau}(s,t) \coloneqq b^{-1}\partial_s \boldsymbol{r}(s,t)$, dimensionless persistence length $l_p = 1/\sqrt{4\kappa}$ in sequence space, and uniform reference tension $\kappa(s) = \kappa = 1$. In contrast, for active kicks with nonuniform activity, we employ a spatially varying $\kappa(s)$ to enforce an ensemble-averaged and hence weak constraint of local inextensibility, $\langle|\boldsymbol{\tau}(s,t)|^2\rangle = 1$. Such weak length constraints are certainly different from strongly enforcing inextensibility on the level of individual trajectories, for example, through elastic constraints, which are known to qualitatively affect tension propagation [58]. These limitations notwithstanding, our simplified theory can provide first insights into the folding and dynamics of polymers driven by temporal patterns of excitations. In the following, for convenience and clarity of these ideas, the main text presents analytical theory in the continuum limit, while the figures show numerical evaluations [59] of the analytical theory for discrete chains as described in the Supplemental Material [60].

To model temporal patterns of active kicks $\boldsymbol{\eta}_a(s,t)$, we introduce an additional stochastic process whereby a scalar memory kernel $\mathcal{G}(s,t)$, with characteristic decorrelation time τ_c, integrates i.i.d. random fluctuations $\boldsymbol{\gamma}(s,t)$, so that $\boldsymbol{\eta}_a(s,t) \coloneqq \int_{-\infty}^{t} d\tau\, \mathcal{G}(s,t-\tau)\boldsymbol{\gamma}(s,\tau)$. We consider excitations over a finite width l_e and covariance $\langle \boldsymbol{\gamma}(s,t)\cdot\boldsymbol{\gamma}(s',t')\rangle = b^2/(\tau_b l_e)e^{-|s-s'|/l_e}\delta(t-t')$. Thus, the ratio l_e/l_p between the excitation width and the polymer persistence length is a key parameter. In the limit $l_e \ll l_p$, excitations are independent along the sequence, whereas for $l_e \gtrsim l_p$, entire segments are kicked in similar directions. For variations in $\mathcal{G}(s,t)$ that are smooth over the excitation width, $\partial_s\mathcal{G} \ll l_e^{-1}\mathcal{G}$, we approximate

$$\langle \boldsymbol{\eta}_a(s,t)\cdot\boldsymbol{\eta}_a(s',t')\rangle = \frac{2b^2}{\tau_b}\frac{1}{2l_e}e^{-\frac{|s-s'|}{l_e}}\hat{\mathcal{C}}\left(\frac{s+s'}{2}, t-t'\right), \quad (2a)$$

with sequence-dependent temporal correlations [61]

$$\hat{\mathcal{C}}(s,t) = \int_0^\infty d\tau\, \mathcal{G}(s,|t|+\tau)\mathcal{G}(s,\tau). \quad (2b)$$

Having quantified how the covariance of the active kicks [45] depends on their temporal patterns, we study two scenarios: (i) heteropolymers assembled from persistent random walkers [37–50], and (ii) polymers subject to temporal sequences (programs) of excitations [Fig. 1].

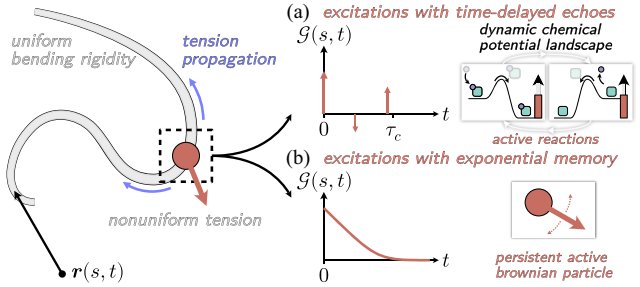

FIG. 1. Sketch of an active semiflexible polymer. Active processes generate excitations, which propagate along the polymer backbone. A nonuniform profile of activity leads to nonuniform line tension, which maintains chain inextensibility. In the present work, we consider two types of excitations: (a) Time-delayed echoes of past kicks at the same location, such as binding followed by unbinding events, and (b) exponentially correlated kicks by persistent self-propelling particles.

To that end, we analyze Eq. (1) via a Rouse mode decomposition [62], with the Fourier transforms $\boldsymbol{r}(s,t) \to \tilde{\boldsymbol{r}}_q(t)$ and $\boldsymbol{\eta}(s,t) \to \tilde{\boldsymbol{\eta}}_q(t)$. We compactify the notation by storing all Rouse modes in a matrix $\boldsymbol{R}(t)$ with rows $R_{q,\ldots}(t) \coloneqq \tilde{\boldsymbol{r}}_q(t)$, and analogously define the excitation matrix $\boldsymbol{H}(t)$ with rows $H_{q,\ldots}(t) \coloneqq \tilde{\boldsymbol{\eta}}_q(t)$. The Fourier-transformed Eq. (1) is solved by

$$\boldsymbol{R}(t) = \int_{-\infty}^{t} d\tau\, e^{-\boldsymbol{J}(t-\tau)}\cdot\boldsymbol{H}(\tau), \quad (3)$$

where the response matrix, $\boldsymbol{J}$, is given by $\tau_b J_{qk} = (1/L)qk\kappa_{q-k} + \frac{1}{4}q^4\delta_{qk}$. We here neglect viscoelastic couplings via the surrounding medium [26,63,64], which can be approximated by an additional memory kernel acting on the backbone velocities, $\partial_t \boldsymbol{r}(s,t)$. Even without taking into account these additional timescales, the interplay between the memory of the excitations and the relaxation time of the polymer already leads to interesting effects.

First, we analyze the dynamics of a polymer subjected to generic excitations with covariance $\boldsymbol{C}(t-t') \coloneqq \langle \boldsymbol{H}(t)\cdot\boldsymbol{H}^\dagger(t')\rangle$ and characteristic decorrelation time τ_c, so that $\boldsymbol{C}(\tau) \sim 0$ for $|\tau| > \tau_c$. In the limit of either long timescales, $|t-t'| > \tau_c$, or in steady state, $t = t' \to \infty$, the memory of the excitations can be effectively integrated out [60], because the polymer has ample time to run through many iterations of the excitation program $\mathcal{G}$. More specifically, the polymer dynamics resemble that of a chain where the excitation program is replaced by couplings between different excitation modes, $\langle \boldsymbol{H}(t)\cdot\boldsymbol{H}^\dagger(t')\rangle \approx \boldsymbol{C}_{\text{eff}}\delta(t-t')$ with

$$\boldsymbol{C}_{\text{eff}} \coloneqq \int_0^\infty d\tau\left[\boldsymbol{C}(\tau)\cdot e^{-\boldsymbol{J}^\dagger\tau} + e^{-\boldsymbol{J}\tau}\cdot\boldsymbol{C}^\dagger(\tau)\right]. \quad (4)$$

The covariance $\boldsymbol{X}(0) \equiv \langle \boldsymbol{R}(t) \cdot \boldsymbol{R}^{\dagger}(t) \rangle$ of the steady-state distribution of conformations is obtained by solving the Lyapunov equation $\boldsymbol{J} \cdot \boldsymbol{X}(0) + \boldsymbol{X}(0) \cdot \boldsymbol{J}^{\dagger} = \boldsymbol{C}_{\mathrm{eff}}$. In the limit where the memory is short-lived, $\tau_c \ll \tau_b$, the polymer fluctuations are well approximated by $\langle \boldsymbol{R}(t) \cdot \boldsymbol{R}^{\dagger}(t') \rangle \approx e^{-\boldsymbol{J}|t-t'|} \cdot \boldsymbol{X}(0)$ for $t > t'$. The complementary case where the memory is long-lived, $\tau_c \gtrsim \tau_b$, however, requires numerical evaluation of the analytical theory. With these tools, we will explore specific models for the response matrix of the polymer, $\boldsymbol{J}$, and for the temporal pattern of excitations encoded in $\boldsymbol{C}(\tau)$.

In the simplest case, on length scales much larger than the excitation width and the persistence length, $\Delta s \gg \max(l_e, l_p)$, tension is expected to propagate predominantly through longitudinal modes. In this limit, it is tempting to approximate $\langle \boldsymbol{\gamma}(s,t) \cdot \boldsymbol{\gamma}(s',t') \rangle \approx (2b^2/\tau_b)\delta(s-s')\delta(t-t')$, drop the bending term in Eq. (1), and set $\kappa(s) = 1$ so that $\tau_b J_{qk} \sim q^2 \delta_{qk}$. Transforming Eq. (4) from Fourier space to sequence space, one finds

$$\frac{\mathcal{C}_{\mathrm{eff}}(s,s')}{2b^2/\tau_b} = \delta(s-s') + \int_0^{\infty} d\tau \frac{\hat{\mathcal{C}}(s,\tau) + \hat{\mathcal{C}}(s',\tau)}{\sqrt{4\pi\tau/\tau_b}} e^{-\frac{(s-s')^2}{4\tau/\tau_b}}, \quad (5)$$

which, as will be illuminated shortly, is a good approximation when $l_e \gg l_p$. Thus, purely local temporal sequences of kicks, which are relayed via the tension of the polymer backbone, can lead to effective sequence-controlled correlated excitations.

This is illustrated in Fig. 2(a) for a discrete flexible chain subjected to inhomogeneous excitations $\mathcal{G}(s,t) = \sqrt{\epsilon(s)}\mathcal{G}_{\pm}(t)$ with echoes [65], $\mathcal{G}_{\pm}(t) = \delta(t) \pm \delta(t-\tau_c)$.

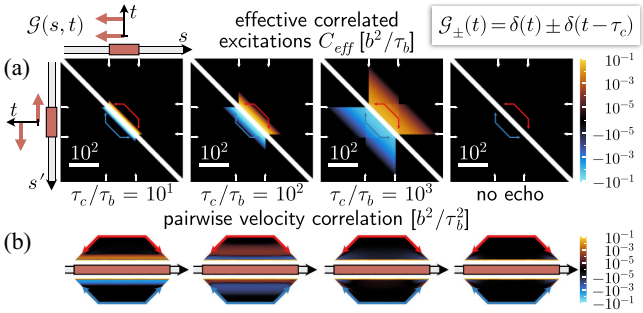

FIG. 2. (a) Local active processes lead to effectively correlated excitations of a 10^3-mer flexible chain. Red arrows indicate that each active kick in the active region ($\epsilon = 1$ for $s \in$ red segment, delimited by white arrows) is followed by a time-lagged positive ($\mathcal{G}_+$, above diagonal) or negative ($\mathcal{G}_-$, below diagonal) echo. Scale bar: 10^2 monomers of size b. (b) Same-time velocity pair correlations, $\langle \boldsymbol{v}^{\delta}(s,t) \cdot \boldsymbol{v}^{\delta}(s',t) \rangle$ with time discretization $\delta = 0.1\tau_b \ll \tau_c$ shorter than the memory. Red and blue outlines correspond to solid lines in (a). Positive (negative) echoes with larger lag time τ_c cause longer-ranged but weaker positive (negative) velocity correlations.

The general effect is identical if the waiting time between an active kick and its echo is not sharp but follows a $\Gamma(n,\lambda)$ distribution arising from an n-step Poisson process with typical step rate λ [60]. Within the lag time τ_c between an active kick and its subsequent echo, forces propagate diffusively across a typical distance $|s-s'| \propto \sqrt{\tau_c/\tau_b}$ [Eq. (5)], effectively coupling the excitations of loci s and s'. Consequently, the locus velocities $\boldsymbol{v}^{\delta}(s,t) := [\boldsymbol{r}(s,t+\delta) - \boldsymbol{r}(s,t)]/\delta$ also exhibit pairwise correlations which are well approximated by $\langle \boldsymbol{v}^{\delta}(s,t) \cdot \boldsymbol{v}^{\delta}(s',t) \rangle \approx \delta^{-1}\mathcal{C}_{\mathrm{eff}}(s,s')$ for $\tau_c \ll \delta \ll \tau_b$. This approximation fails if the time discretization δ is too fine to integrate out the memory, i.e., when $\delta \ll \tau_c$. Nevertheless, when compared to an explicit evaluation of the pairwise velocity correlations, $\mathcal{C}_{\mathrm{eff}}(s,s')$ reasonably predicts which regions show coordinated motion [left two panels in Fig. 2(b)]. As discussed in our prior work [19], because correlated (anticorrelated) excitations imply effective attraction (repulsion) between loci, Eq. (5) also informs about the conformations of the polymer.

To further elucidate the results so far, we revisit a scenario where the excitations have exponential memory, $\mathcal{G}(s,t) = \sqrt{\epsilon(s)}\tau_c^{-1} e^{-|t|/\tau_c}$, which has been the focus of several theoretical studies [37–49] and reviewed in Refs. [61]. Diffusive propagation of tension through lateral stretching modes [Eq. (5)] leads to

$$\frac{\mathcal{C}_{\mathrm{eff}}(s,s')}{2b^2/\tau_b} = \delta(s-s') + \frac{\epsilon(s) + \epsilon(s')}{4l_e} e^{-\frac{|s-s'|}{l_e}}, \quad (6)$$

with $l_e := \sqrt{\tau_c/\tau_b}$. For flexible chains, a local increase in activity should then lead to swelling [19,50]. Semiflexible active chains, however, can show either swelling *or contraction* with increasing activity [50]. To reconcile these results, one needs to take into account the propagation of transversal excitation modes via bending.

Assuming large and nearly uniform activity along the semiflexible polymer, $\epsilon(s) \gg 1$ and $\partial_s \epsilon(s) \ll l_e^{-1}\epsilon(s)$, the exponential memory can be replaced by memoryless noise of the form $\mathcal{G}(s,t) = \sqrt{\epsilon(s)}\delta(t)$ and a renormalized excitation width $l_e \approx l_e$ in Eq. (2). We determine the local Lagrange multiplier $\kappa(s)$ from the weak constraint $\langle |\boldsymbol{\tau}(s,t)|^2 \rangle = 1$, as shown in the Supplemental Material [60]. On large length scales (i.e., for long wave modes), the dynamics of the semiflexible polymer are approximately given by

$$\tau_b[\partial_t \boldsymbol{r}(s,t) - \boldsymbol{\eta}(s,t)] = \partial_s \left[\left(1 + \frac{2\epsilon(s)}{1+2l_e} \right) \partial_s \boldsymbol{r}(s,t) \right], \quad (7)$$

where activity introduces tension modulations as derived in the Supplemental Material [60]. Thus, treating the polymer as an effective Rouse chain is internally consistent if the excitations decorrelate over distances much larger than the

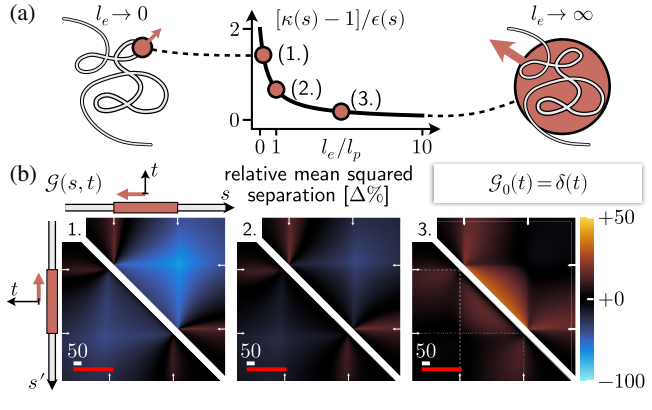

FIG. 3. The excitation width l_e determines the response of the semiflexible chain. (a) Narrow kicks (left) agitate bending modes and thereby increase the local tension of a specific segment [Eq. (7)]. The limit of broad kicks (right) recovers a flexible chain with uniform tension. (b) Change in pairwise squared separation compared to a passive chain, as induced by memoryless active kicks in an active region ($\epsilon = 0.5$ for $s \in$ red segment, delimited by white arrows). Above diagonal: Macroscopic ($|s - s'| \gg l_{e,p}$) behavior of continuous wormlike chain. Below diagonal: 10^3-mer semiflexible chain, where scale bars indicate 50 monomers (white) or persistence lengths (red). (1.) For $l_e \to 0$, agitation of bending modes *compacts* the polymer. (2.) For $l_e = l_p$, the active polymer resembles an *inextensible flexible* chain. (3.) For $l_e \to \infty$, agitation of stretching modes leads to Rouse chain behavior.

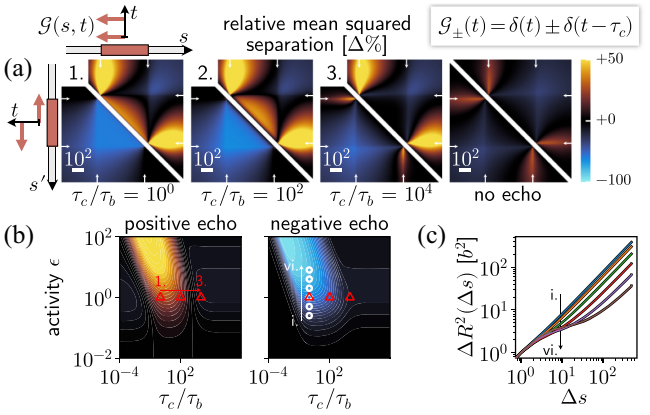

FIG. 4. Response of an inextensible 10^3-mer flexible chain to active processes. (a) Change in pairwise squared separation compared to a uniform chain. Red arrows illustrate that each kick in the active region ($\epsilon = 1$ for $s \in$ red segment, delimited by white arrows) is followed by a time-lagged positive ($\mathcal{G}_+$, above diagonal) or negative ($\mathcal{G}_-$, below diagonal) echo. Scale bar: 10^2 monomers of size b. (b) Average change in pairwise separation within the active segment as a function of the activity ϵ and the echo lag time. Time-delayed echoes show the strongest effect for intermediate time lags ($\tau_c \sim \tau_b$). In the limits $\tau_c \ll \tau_b$ or $\tau_c \gg \tau_b$, excitations become statistically independent. Red triangles correspond to mean squared separation maps in (a) and (c). Mean squared distance from the center monomer in a homogeneous inextensible flexible chain driven by kicks with echoes; parameters are indicated by white circles in (b). Negative echoes decrease the radius of gyration by introducing a regime where the curves plateau (black arrow).

persistence length [Fig. 3(b)]. Then, large coiled segments (Pincus blobs [66]) experience coherent excitations, primarily leading to agitation of longitudinal modes.

In general, however, Eq. (7) demonstrates that regions with locally increased activity also show an increased tension of the polymer backbone. For cases where the excitations occur on length scales smaller than a Pincus blob, $l_e < l_p$, this can qualitatively change the response of the polymer by causing active segments to contract instead of expanding [above the diagonal in Fig. 3(b)]. These continuum theory predictions also apply to discrete semiflexible chains [below the diagonal in Fig. 3(b)], where the response matrix is described in the Supplemental Material [60] and in Refs. [67,68]. The underlying mechanism is that, for $l_e \ll l_p$, excitations primarily agitate bending modes in a given polymer segment and, since segment length is conserved, reduce its end-to-end distance analogous to an entropic spring. In contrast, for $l_e \gg l_p$, excitations cannot agitate bending modes and instead agitate long distance modes along the polymer segment. Thus, the interplay between features of the excitations and the microscopic mechanics of the polymer can determine if active regions expand ($l_e > l_p$) or contract ($l_e < l_p$). Extrapolating these results, the persistence time τ_c of active particles can control if semiflexible chains swell or contract [50].

In light of these results, we now revisit the scenario of an inextensible polymer subject to temporal sequences of kicks. For simplicity, we focus on length scales much larger than the excitation width and the persistence length, which we take to be comparable $l_e \sim l_p$. In this limit, our results on memoryless excitations suggest that we can approximate the active wormlike chain as an inextensible flexible polymer. As shown in Fig. 4(a), activity-induced bending [19], combined with the constraint of chain inextensibility, drastically reduces the mean squared separation between the boundaries of the active region. Moreover, positive echoes deplete contacts within this active domain [above the diagonal in Fig. 4(a)], which is indicative of a looplike state. Conversely, negative echoes enhance contacts and can even induce compaction by almost 100%, reminiscent of a coil-to-globule transition [below the diagonal in Fig. 4(a)]. Since similar effects can, on smaller scales, be observed for semiflexible polymers [60], we conclude that inextensibility has a defining role for polymer dynamics.

In summary, we have analyzed the conformations and dynamics of a broad class of inhomogeneous active polymers which experience local temporal patterns of excitations. Within this theoretical framework, different segments can vary in activity, persistence time, or even

show unique temporal excitation programs. For example, a sequence of active pushing and binding, followed by an elastic recoil or pulling on a specific locus, will have characteristic temporal correlations with negative echoes, which can be viewed as time-delayed analogs of local force dipoles. This could also apply to the extrusion of chromatin loops [69]: if the forces exerted by the cohesin motor at a loop anchor propagate along the clamped chromatin loop until they return to the loop anchor, there will be effective positive echoes. Finally, we hypothesize that similar time-delayed echoes may also arise from the interaction forces during nonequilibrium chemical reaction cycles, where a protein first exothermically binds to a monomer, undergoes a conformational change, and finally exothermically unbinds. These qualitative features of the excitations (such as negative or positive echoes) and quantitative properties (delay times of the echoes) determine which regions of the polymer move coherently and how the active segment folds. Moreover, our framework can explain previous theoretical observations of polymer swelling and collapse [39–43,50] as a competition between (a) the polymer persistence length, and (b) the typical arc distance that excitations are relayed through tension propagation along the polymer backbone. We hypothesize that such a competition of length scales could be relevant for biopolymers such as chromatin, and could determine if active segments expand or collapse.

Acknowledgments—We thank Arup K. Chakraborty for engaging in insightful discussions. This work was supported by the National Science Foundation, through the Biophysics of Nuclear Condensates Grant No. MCB-2044895. A. G. was also supported by an EMBO Postdoctoral Fellowship No. ALTF 259-2022. D. K. was supported by the Graduate Research Fellowship Program under Grant No. 2141064. The authors acknowledge the MIT SuperCloud and Lincoln Laboratory Supercomputing Center for providing HPC resources that have contributed to the research results reported within this paper.

[1] J. N. Onuchic, Z. Luthey-Schulten, and P. G. Wolynes, Annu. Rev. Phys. Chem. **48**, 545 (1997).
[2] V. S. Pande, A. Y. Grosberg, and T. Tanaka, Rev. Mod. Phys. **72**, 259 (2000).
[3] E. Shakhnovich, Chem. Rev. **106**, 1559 (2006).
[4] K. A. Dill, S. B. Ozkan, M. S. Shell, and T. R. Weikl, Annu. Rev. Biophys. **37**, 289 (2008).
[5] P. G. Wolynes, Biochimie **119**, 218 (2015).
[6] R. Nassar, G. L. Dignon, R. M. Razban, and K. A. Dill, J. Mol. Biol. **433**, 167126 (2021).
[7] J. L. England and V. S. Pande, Biophys. J. **95**, 3391 (2008).
[8] J. L. England, Structure **19**, 967 (2011).
[9] N. Perunov and J. L. England, Protein Sci. **23**, 387 (2014).
[10] T. Misteli, Cell **183**, 28 (2020).
[11] S. C. Weber, A. J. Spakowitz, and J. A. Theriot, Proc. Natl. Acad. Sci. U.S.A. **109**, 7338 (2012).
[12] A. Zidovska, D. A. Weitz, and T. J. Mitchison, Proc. Natl. Acad. Sci. U.S.A. **110**, 15555 (2013).
[13] M. P. Backlund, R. Joyner, K. Weis, and W. E. Moerner, Mol. Biol. Cell **25**, 3619 (2014).
[14] H. A. Shaban, R. Barth, and K. Bystricky, Nucleic Acids Res. **46**, e77 (2018).
[15] J. Halatek, F. Brauns, and E. Frey, Phil. Trans. R. Soc. B **373**, 20170107 (2018).
[16] G. J. Narlikar, R. Sundaramoorthy, and T. Owen-Hughes, Cell **154**, 490 (2013).
[17] F. Uhlmann, Nat. Rev. Mol. Cell Biol. **17**, 399 (2016).
[18] M. A. Reid, Z. Dai, and J. W. Locasale, Nat. Cell Biol. **19**, 1298 (2017).
[19] A. Goychuk, D. Kannan, A. K. Chakraborty, and M. Kardar, Proc. Natl. Acad. Sci. U.S.A. **120**, e2221726120 (2023).
[20] G. Le Treut, F. Képès, and H. Orland, Biophys. J. **115**, 2286 (2018).
[21] G. Shi and D. Thirumalai, Nat. Commun. **10**, 3894 (2019).
[22] B. Zhang and P. G. Wolynes, Biophys. J. **112**, 427 (2017).
[23] M. Di Pierro, D. A. Potoyan, P. G. Wolynes, and J. N. Onuchic, Proc. Natl. Acad. Sci. U.S.A. **115**, 7753 (2018).
[24] C. P. Brangwynne, G. H. Koenderink, F. C. MacKintosh, and D. A. Weitz, Trends Cell Biol. **19**, 423 (2009).
[25] F. S. Gnesotto, F. Mura, J. Gladrow, and C. P. Broedersz, Rep. Prog. Phys. **81**, 066601 (2018).
[26] T. J. Lampo, A. S. Kennard, and A. J. Spakowitz, Biophys. J. **110**, 338 (2016).
[27] S. Put, T. Sakaue, and C. Vanderzande, Phys. Rev. E **99**, 032421 (2019).
[28] H. Salari, M. Di Stefano, and D. Jost, Genome Res. **32**, 28 (2022).
[29] L. Liu, G. Shi, D. Thirumalai, and C. Hyeon, PLoS Comput. Biol. **14**, e1006617 (2018).
[30] Z. Jiang, Y. Qi, K. Kamat, and B. Zhang, J. Phys. Chem. B **126**, 5619 (2022).
[31] R. Bruinsma, A. Y. Grosberg, Y. Rabin, and A. Zidovska, Biophys. J. **106**, 1871 (2014).
[32] I. Eshghi, A. Zidovska, and A. Y. Grosberg, Phys. Rev. Lett. **131**, 048401 (2023).
[33] F. C. MacKintosh and A. J. Levine, Phys. Rev. Lett. **100**, 018104 (2008).
[34] D. Saintillan, M. J. Shelley, and A. Zidovska, Proc. Natl. Acad. Sci. U.S.A. **115**, 11442 (2018).
[35] A. Mahajan, W. Yan, A. Zidovska, D. Saintillan, and M. J. Shelley, Phys. Rev. X **12**, 041033 (2022).
[36] S. Chaki, L. Theeyancheri, and R. Chakrabarti, Soft Matter. **19**, 1348 (2023).
[37] A. Ghosh and N. S. Gov, Biophys. J. **107**, 1065 (2014).
[38] A. Kaiser, S. Babel, B. ten Hagen, C. von Ferber, and H. Löwen, J. Chem. Phys. **142**, 124905 (2015).
[39] T. Eisenstecken, G. Gompper, and R. G. Winkler, Polymers **8**, 304 (2016).
[40] T. Eisenstecken, A. Ghavami, A. Mair, G. Gompper, and R. G. Winkler, AIP Conf. Proc. **1871**, 050001 (2017).
[41] S. M. Mousavi, G. Gompper, and R. G. Winkler, J. Chem. Phys. **150**, 064913 (2019).
[42] S. K. Anand and S. P. Singh, Phys. Rev. E **101**, 030501(R) (2020).
[43] S. Brahmachari, T. Markovich, F. C. MacKintosh, and J. N. Onuchic, PRX Life **2**, 033003 (2024).

[44] T. Eisenstecken, G. Gompper, and R. G. Winkler, J. Chem. Phys. **146**, 154903 (2017).
[45] D. Osmanović and Y. Rabin, Soft Matter **13**, 963 (2017).
[46] D. Osmanović, J. Chem. Phys. **149**, 164911 (2018).
[47] T. Saito and T. Sakaue, Polymers **11**, 2 (2019).
[48] A. Ghosh and A. J. Spakowitz, Phys. Rev. E **105**, 014415 (2022).
[49] A. Ghosh and A. J. Spakowitz, Soft Matter **18**, 6629 (2022).
[50] R. G. Winkler and G. Gompper, J. Chem. Phys. **153**, 040901 (2020).
[51] S. Dutta, A. Ghosh, and A. J. Spakowitz, Soft Matter **20**, 1694 (2024).
[52] A. Goychuk, L. Demarchi, I. Maryshev, and E. Frey, Phys. Rev. Research **6**, 033082 (2024).
[53] M. M. Hanczyc, Phil. Trans. R. Soc. B **366**, 2885 (2011).
[54] M. Dindo, A. Bevilacqua, G. Soligo, A. Monti, M. E. Rosti, and P. Laurino, J. Am. Chem. Soc. **146**, 15965 (2024).
[55] E. Jambon-Puillet, A. Testa, C. Lorenz, R. W. Style, A. A. Rebane, and E. R. Dufresne, Nat. Commun. **15**, 3919 (2024).
[56] H. H. Schede, P. Natarajan, A. K. Chakraborty, and K. Shrinivas, Nat. Commun. **14**, 4152 (2023).
[57] L. Demarchi, A. Goychuk, I. Maryshev, and E. Frey, Phys. Rev. Lett. **130**, 128401 (2023).
[58] O. Hallatschek, E. Frey, and K. Kroy, Phys. Rev. E **75**, 031905 (2007).
[59] A. Goychuk, D. Kannan, and M. Kardar, Source Code-Delayed Excitations Induce Polymer Looping and Coherent Motion (2024), 10.5281/zenodo.13201207.
[60] See Supplemental Material at http://link.aps.org/supplemental/10.1103/PhysRevLett.133.078101 for details of the analytical and numerical calculations.
[61] K. Goswami, S. Chaki, and R. Chakrabarti, J. Phys. A **55**, 423002 (2022).
[62] P. E. Rouse, J. Chem. Phys. **21**, 1272 (1953).
[63] S. C. Weber, A. J. Spakowitz, and J. A. Theriot, Phys. Rev. Lett. **104**, 238102 (2010).
[64] S. C. Weber, J. A. Theriot, and A. J. Spakowitz, Phys. Rev. E **82**, 011913 (2010).
[65] We consider the Dirac δ distribution to be asymmetric, and define $\int_0^\infty dx\,\delta(x) = 1$.
[66] M. Rubinstein and R. H. Colby, *Polymer Physics* (Oxford University Press, Oxford, 2003).
[67] R. G. Winkler, J. Chem. Phys. **118**, 2919 (2003).
[68] A. R. Tejedor, J. R. Tejedor, and J. Ramírez, J. Chem. Phys. **157**, 164904 (2022).
[69] E. J. Banigan and L. A. Mirny, Curr. Opin. Cell Biol. **64**, 124 (2020).